Extension of the Sliced Gaussian Mixture Filter with Application to Cooperative Passive Target Tracking

Julian Hörst, Felix Sawo,
Vesa Klumpp, Uwe D. Hanebeck
Intelligent Sensor-Actuator-Systems Laboratory (ISAS),
Institute for Anthropomatics,
Universität Karlsruhe (TH), Germany.
{hoerst,sawo,klumpp}@ira.uka.de, uwe.hanebeck@ieee.org

Dietrich Fränken

Data Fusion Algorithms and Software
EADS Deutschland GmbH
D-89077 Ulm, Germany
dietrich.fraenken@eads.com

Abstract – *This paper copes with the problem of nonlinear Bayesian state estimation. A nonlinear filter, the Sliced Gaussian Mixture Filter (SGMF), employs linear substructures in the nonlinear measurement and prediction model in order to simplify the estimation process. Here, a special density representation, the sliced Gaussian mixture density, is used to derive an exact solution of the Chapman-Kolmogorov equation. The sliced Gaussian mixture density is obtained by a systematic and deterministic approximation of a continuous density minimizing a certain distance measure. In contrast to previous work, improvements of the SGMF presented here include an extended system model and the processing of multi-dimensional nonlinear subspaces. As an application for the SGMF, cooperative passive target tracking, where sensors take angular measurements from a target, is considered in this paper. Finally, the performance of the proposed estimator is compared to the marginalized particle filter (MPF) in simulations.*

Keywords: Bearings-only tracking, nonlinear estimation, Rao-Blackwellization, Gaussian mixture, Dirac mixture

1 Introduction

Stochastic state estimation has a variety of applications, including vehicle localization, speech processing, SLAM, or target tracking [1]. For special cases of linear systems and Gaussian densities, state estimation can be performed analytically with the well-known Kalman filter. In case of nonlinear system models, modifications to the Kalman filter, like the extended Kalman filter or the unscented Kalman filter [2], exist. The results of the unscented Kalman filter can be improved by a more sophisticated sample selection from the Gaussian density, as shown in the Gauss filter [3]. All the above mentioned estimators have in common that the estimated density is represented by a Gaussian. Another well-known density representation is by means of samples, as employed in particle filters [4]. Their advantage lies in very simple processing, even for nonlinear systems. One major drawback is that many samples may be needed, which can become very computationally demanding, and thus, intractable for high-dimensional problems.

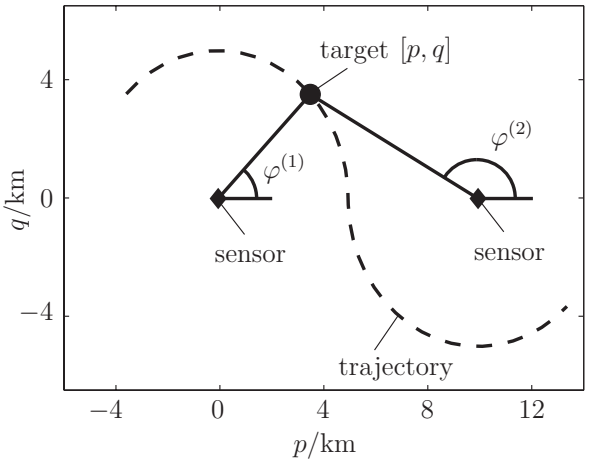

Figure 1: Visualization of cooperative passive target tracking with angular measurements.

In the special case of mixed linear/nonlinear systems, the Sliced Gaussian Mixture Filter [5] can be used. Here, linear substructures in the system and measurement model are employed. This so-called Rao-Blackwellization leads to conditionally linear estimation problems, which can be handled efficiently, even for high-dimensional state-spaces. This principle is also applied in the marginalized (or Rao-Blackwellized) particle filter [6]. Rao-Blackwellization is especially advantageous for high-dimensional linear parts and low-dimensional nonlinear parts as, e. g., for simultaneous parameter and state estimation [6, 7].

Another application, which is regarded in this paper, is *cooperative passive target tracking* with angular measurements [1], also known as bearings-only tracking. Considering this application, the proposed estimator will be compared to the marginalized particle filter that has already been employed in this context [8].

Fig. 1 shows the principle of cooperative passive target tracking: The sensors try to track a target with an unknown trajectory by measuring angles to the target. It is only possible to determine the location of the target by measurements from different sensor positions, which can be done either

with multiple or movable sensors. Within this paper, we assume that measurements are taken by two dislocated stationary measurement devices.

The novelties of this paper include several enhancements of the Sliced Gaussian Mixture Filter. Multi-dimensional nonlinear problems can be considered by a systematic density approximation. Furthermore, the capability to cope with correlated Gaussian system noise and extensions of the system model allow a wider range of applications.

The paper is structured as follows: In the next section, the concept of conditionally linear systems is outlined and the considered system and measurement models are described. In Section 3, the Sliced Gaussian Mixture Filter and the new modifications are stated. Section 4 gives a short introduction to cooperative passive target tracking. The performance of the proposed filter is shown in Section 5. Here, the SGMF is compared to the marginalized particle filter in a cooperative passive target tracking simulation.

2 Problem Formulation

The main goal of an estimator is to obtain an accurate estimation of the system state $\underline{x}_k \in \Omega$ at every discrete time step k in terms of a density function $f(\underline{x}_k)$. For estimation, a model of the system's dynamic behaviour is needed. If this model is based on general system equations and arbitrary density functions, the estimation problem can only be solved approximatively.

However, for special types of systems, linear substructures can be exploited for a more efficient estimation process. This method is known as Rao-Blackwellization [9]. The key idea here is to decompose the estimation problem by dividing the state vector into a *nonlinear substate* $\underline{x}_k^n \in \mathbb{R}^s$ and a *linear substate* $\underline{x}_k^l \in \mathbb{R}^r$.

In this paper, we assume the following structure of the discrete-time *system model*, as proposed in [6],

$$\begin{aligned} \underline{\boldsymbol{x}}_{k+1}^l &= \mathbf{A}_k^l(\underline{\boldsymbol{x}}_k^n)\underline{\boldsymbol{x}}_k^l + \underline{a}_k^l(\underline{\boldsymbol{x}}_k^n) + \underline{\boldsymbol{w}}_k^l \\ \underline{\boldsymbol{x}}_{k+1}^n &= \mathbf{A}_k^n(\underline{\boldsymbol{x}}_k^n)\underline{\boldsymbol{x}}_k^l + \underline{a}_k^n(\underline{\boldsymbol{x}}_k^n) + \underline{\boldsymbol{w}}_k^n \quad , \end{aligned} \tag{1}$$

where the noise terms $\underline{\boldsymbol{w}}_k^l$ and $\underline{\boldsymbol{w}}_k^n$ are zero mean, white, and Gaussian distributed with the following covariance matrix

$$\mathrm{Cov}\left\{\begin{bmatrix}\underline{\boldsymbol{w}}_k^l \\ \underline{\boldsymbol{w}}_k^n\end{bmatrix}\right\} = \mathbf{C}_k^w = \begin{bmatrix}\mathbf{C}_k^{wll} & \mathbf{C}_k^{wln} \\ \mathbf{C}_k^{wnl} & \mathbf{C}_k^{wnn}\end{bmatrix} .$$

Note that throughout this paper, random variables are denoted by bold face lower-case letters. The system matrices $\mathbf{A}_k^l(\,\cdot\,)$ and $\mathbf{A}_k^n(\,\cdot\,)$ for the linear and nonlinear subspace depend on the nonlinear substate vector $\underline{x}_k^n$. The nonlinear part of the system model is represented by $\underline{a}_k^l(\,\cdot\,)$ and $\underline{a}_k^n(\,\cdot\,)$, respectively. Furthermore, the *measurement model* is given by

$$\underline{\hat{y}}_k = \mathbf{H}_k(\underline{\boldsymbol{x}}_k^n)\underline{\boldsymbol{x}}_k^l + \underline{h}_k(\underline{\boldsymbol{x}}_k^n) + \underline{\boldsymbol{v}}_k \quad , \tag{2}$$

where $\underline{\hat{y}}_k$ is the measurement at time step k. Here, the noise term $\underline{\boldsymbol{v}}_k$ is assumed to be white and Gaussian distributed with zero mean and covariance matrix $\mathbf{C}_k^v$. The measurement matrix $\mathbf{H}_k(\,\cdot\,)$ depends on the nonlinear substate $\underline{x}_k^n$ and $\underline{h}_k(\,\cdot\,)$ represents the nonlinear dependency.

For these systems, the estimation problem for one filter and prediction step can be solved analytically by employing a special density representation, the sliced Gaussian mixture density. This density was introduced in [5], where the processing of a more restricted model was discussed.

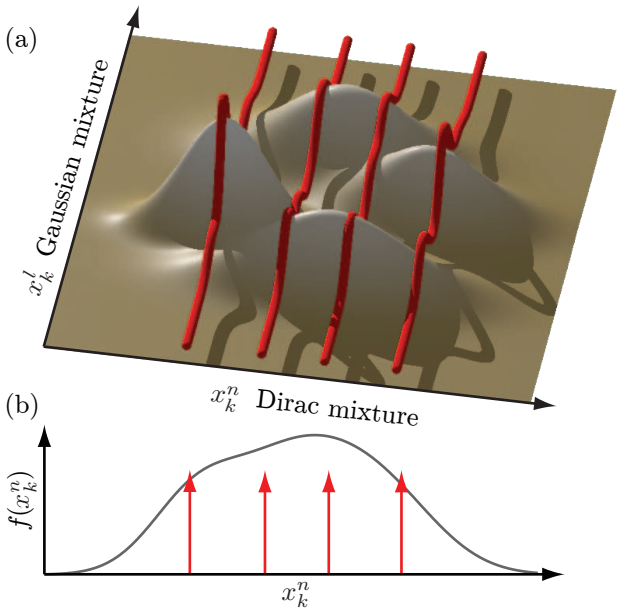

Figure 2: Density approximation: (a) A Gaussian mixture density over the complete state space is approximated by a sliced Gaussian mixture density. (b) Marginal density over the nonlinear subspace, which is approximated by a Dirac mixture density.

3 The Sliced Gaussian Mixture Filter

In this section, we review the Sliced Gaussian Mixture Filter (SGMF) as described in [5]. In addition, several extensions are introduced that are necessary for the application to cooperative passive target tracking. These extensions include:

- A more general structure of the system model allowing for a wider range of applications,
- system noise correlated between the linear and nonlinear subspace,
- and the handling of a multi-dimensional nonlinear subspace during the density approximation.

3.1 Density representation

By using a special density representation, the estimation problem based on the nonlinear system (1) and (2) can be decomposed into a (conditionally) linear and a nonlinear problem. This density function consists of a *Dirac mixture* in the nonlinear subspace $\underline{x}_k^n$ and a *Gaussian mixture* in the linear subspace $\underline{x}_k^l$. To be more specific, the so-called *sliced Gaussian mixture density* is represented as follows:

$$f(\underline{x}_k^l, \underline{x}_k^n) = \sum_{i=1}^{M} \alpha_k^i \underbrace{\delta(\underline{x}_k^n - \underline{\xi}_k^i)}_{\text{Dirac mixture}} \underbrace{f(\underline{x}_k^l | \underline{\xi}_k^i)}_{\text{Gaussian mixture}} \quad , \tag{3}$$

where $\delta(\,\cdot\,)$ denotes the Dirac delta distribution. The scalar M represents the number of density slices and $\underline{\xi}_k^i \in \mathbb{R}^s$ can be regarded as the positions of the individual density slices.

Table 1: **Filter Step**: Parameters of the estimated density.

Conditionally linear subspace
$\gamma_k^{ij} \leftarrow \mathcal{N}\Big(\hat{\underline{y}}_k - \mathbf{H}_k^i \underline{\mu}_k^{lij} - \underline{h}_k(\underline{\xi}_k^i), \mathbf{H}_k^i \mathbf{C}_k^{lij} \mathbf{H}_k^{i\,\mathrm{T}} + \mathbf{C}_k^v\Big)$
$\underline{\mu}_k^{lij} \leftarrow \underline{\mu}_k^{lij} + \mathbf{K}_k \left(\hat{\underline{y}}_k - \mathbf{H}_k^i \underline{\mu}_k^{lij} - \underline{h}_k(\underline{\xi}_k^i)\right)$
$\mathbf{C}_k^{lij} \leftarrow \mathbf{C}_k^{lij} - \mathbf{K}_k \mathbf{H}_k^i \mathbf{C}_k^{lij}$
with $\mathbf{K}_k = \mathbf{C}_k^{lij} \mathbf{H}_k^{i\,\mathrm{T}} \left(\mathbf{C}_k^v + \mathbf{H}_k^i \mathbf{C}_k^{lij} \mathbf{H}_k^{i\,\mathrm{T}}\right)^{-1}$

Table 2: **Prediction Step**: Parameters of the predicted density.

Cond. linear subspace	Nonlinear subspace
$\underline{\mu}_{k+1}^{lij} \leftarrow \mathbf{A}_k^{li} \underline{\mu}_k^{lij} + \underline{a}_k^l(\underline{\xi}_k^i)$	$\underline{\mu}_{k+1}^{nij} \leftarrow \mathbf{A}_k^{ni} \underline{\mu}_k^{lij} + \underline{a}_k^n(\underline{\xi}_k^i)$
$\mathbf{C}_{k+1}^{ij} \leftarrow \begin{bmatrix} \mathbf{A}_k^{li} \mathbf{C}_k^{lij} \mathbf{A}_k^{li\,\mathrm{T}} & \mathbf{A}_k^{li} \mathbf{C}_k^{lij} \mathbf{A}_k^{ni\,\mathrm{T}} \\ \mathbf{A}_k^{ni} \mathbf{C}_k^{lij} \mathbf{A}_k^{li\,\mathrm{T}} & \mathbf{A}_k^{ni} \mathbf{C}_k^{lij} \mathbf{A}_k^{ni\,\mathrm{T}} \end{bmatrix} + \mathbf{C}_k^w$	

Discrete marginal density The marginal density function characterizing the system state in the nonlinear subspace is given by the following *Dirac mixture density*:

$$f(\underline{x}_k^n) = \sum_{i=1}^{M} \alpha_k^i \delta(\underline{x}_k^n - \underline{\xi}_k^i), \quad \sum_{i=1}^{M} \alpha_k^i = 1 \ , \tag{4}$$

where $\alpha_k^i \in \mathbb{R}_+$ and $\underline{\xi}_k^i \in \mathbb{R}^s$ are the weights and positions of the Dirac distribution $\delta(\,\cdot\,)$. Conditioned on a particular value of the nonlinear subspace, the estimation problem turns out to be a linear problem. Roughly speaking, for a set of discrete values for $\underline{\boldsymbol{x}}_k^n$, the estimation problem can be solved by a set of linear estimators as shown in Sec. 3.2.

Continuous marginal density In general, the density along the individual slices can be represented by any continuous density function. In this work, Gaussian mixture densities are employed as a universal approximator for arbitrary density functions. The density function for the linear subspace $\underline{x}_k^l$ is given by

$$f(\underline{x}_k^l | \underline{\xi}_k^i) = \sum_{j=1}^{N^i} \beta_k^{ij} \mathcal{N}\Big(\underline{x}_k^l - \underline{\mu}_k^{lij}, \mathbf{C}_k^{lij}\Big), \quad \sum_{j=1}^{N^i} \beta_k^{ij} = 1 \ , \tag{5}$$

with $\beta_k^{ij} \in \mathbb{R}_+$, $\underline{\mu}_k^{lij} \in \mathbb{R}^r$, $\mathbf{C}_k^{lij} \in \mathbb{R}^{r \times r}$ denoting the conditional weight, conditional mean and conditional covariance matrix of the j-th component of the attached Gaussian mixture density of the i-th slice. Here, it is important to emphasize that all the density parameters are conditioned on the location $\underline{\xi}_k^i$ of the density slices.

3.2 Filter and Prediction Step

In this section, the equations for a combined filter and prediction step are derived. The filter step is performed on a sliced Gaussian mixture density, followed by the prediction step. The predicted density $\widetilde{f}^p(\underline{x}_{k+1}^l, \underline{x}_{k+1}^n)$ for the next discrete time step $k+1$ can be determined by substituting Bayes' formula into the Chapman-Kolmogorov equation, according to

$$\widetilde{f}^p(\underline{x}_{k+1}) = \int_{\Omega} f^T(\underline{x}_{k+1} | \underline{x}_k) \underbrace{c_k \cdot f^L(\hat{\underline{y}}_k | \underline{x}_k) f^p(\underline{x}_k)}_{f^e(\underline{x}_k)} \mathrm{d}\underline{x}_k \ .$$

In view of the system model (1) and the measurement model (2), the transition density $f^T(\,\cdot\,)$ and likelihood $f^L(\,\cdot\,)$ are given by

$$f^T(\underline{x}_{k+1} | \, \underline{x}_k) = \mathcal{N}\left(\begin{bmatrix} \underline{x}_{k+1}^l - \mathbf{A}_k^l(\underline{x}_k^n) \underline{x}_k^l - \underline{a}_k^l(\underline{x}_k^n) \\ \underline{x}_{k+1}^n - \mathbf{A}_k^n(\underline{x}_k^n) \underline{x}_k^l - \underline{a}_k^n(\underline{x}_k^n) \end{bmatrix}, \mathbf{C}_k^w \right)$$

$$f^L(\hat{\underline{y}}_k | \, \underline{x}_k) = \mathcal{N}\Big(\hat{\underline{y}}_k - \mathbf{H}_k(\underline{x}_k^n) \underline{x}_k^l - \underline{h}_k(\underline{x}_k^n), \mathbf{C}_k^v\Big) \ .$$

The prior density function $f^p(\underline{x}_k)$ at time step k is represented by a sliced Gaussian mixture according to (3) that consists of a conditional Gaussian mixture in the linear subspace described in equation (5). This leads to

$$\widetilde{f}^p\big(\underline{x}_{k+1}\big) = c_k \int_{\mathbb{R}^r} \int_{\mathbb{R}^s} f^T(\underline{x}_{k+1}^l, \underline{x}_{k+1}^n | \, \underline{x}_k^l, \underline{x}_k^n) f^L(\hat{\underline{y}}_k | \, \underline{x}_k^l, \underline{x}_k^n)$$
$$\sum_{i=1}^{M} \alpha_k^i \delta(\underline{x}_k^n - \underline{\xi}_k^i) \sum_{j=1}^{N^i} \beta_k^{ij} \mathcal{N}\Big(\underline{x}_k^l - \underline{\mu}_k^{lij}, \mathbf{C}_k^{lij}\Big) \, \mathrm{d}\underline{x}_k^n \, \mathrm{d}\underline{x}_k^l \tag{6}$$

with a normalization constant c_k.

Applying the sifting property of Dirac's delta distribution to (6) results in the following Gaussian mixture density $\widetilde{f}^p(\,\cdot\,)$ at time step $k+1$

$$\widetilde{f}^p\big(\underline{x}_{k+1}\big) = \sum_{i=1}^{M} \sum_{j=1}^{N^i} \nu_{k+1}^{ij} \mathcal{N}\left(\begin{bmatrix} \underline{x}_{k+1}^l - \underline{\mu}_{k+1}^{lij} \\ \underline{x}_{k+1}^n - \underline{\mu}_{k+1}^{nij} \end{bmatrix}, \mathbf{C}_{k+1}^{ij} \right) \ , \tag{7}$$

where the weighting coefficients ν_k^{ij} can be derived by

$$\nu_{k+1}^{ij} = \alpha_k^i \beta_k^{ij} \gamma_k^{ij} \Big/ \left(\textstyle\sum_{i=1}^{M} \sum_{j=1}^{N^i} \alpha_k^i \beta_k^{ij} \gamma_k^{ij} \right) \ .$$

The means $\underline{\mu}_{k+1}^{lij}$ and $\underline{\mu}_{k+1}^{nij}$ and the covariance matrix $\mathbf{C}_{k+1}^{ij}$ are given in Table 1 and Table 2 and described in more detail in the following. In order to keep the equations short, the following abbreviations are used:

$$\mathbf{A}_k^{li} := \mathbf{A}_k^l(\underline{\xi}_k^i), \quad \mathbf{A}_k^{ni} := \mathbf{A}_k^n(\underline{\xi}_k^i), \quad \mathbf{H}_k^i := \mathbf{H}_k(\underline{\xi}_k^i) \ .$$

Filter Step In the filter step, the Gaussian components of the slices are updated according to the likelihood. For fixed $\underline{x}_k^n$, the problem is linear, and thus, the posterior density can be calculated according to the Kalman filter equations. The estimated mean $\underline{\mu}_k^{lij}$, the estimated covariance $\mathbf{C}_k^{lij}$, and the new weights γ_k^{ij} are shown in Table 1. After the filter step, the density representation is still in sliced Gaussian mixture form. If there is no measurement, γ_k^{ij} will be equal to 1 and $\underline{\mu}_k^{lij}, \mathbf{C}_k^{lij}$ remain unchanged.

Prediction Step In Table 2, the predicted means $\underline{\mu}_{k+1}^{lij}$ in the linear subspace and $\underline{\mu}_{k+1}^{nij}$ in the nonlinear subspace for the next discrete time step $k+1$ are given. Here, the slices are converted to a Gaussian mixture (7) over the complete

state space, according to the system model.

3.3 Reapproximation Step

In order to perform the processing in a recursive way, the Gaussian mixture density (7) resulting from the combined filter and prediction step must be *reapproximated* by a sliced Gaussian mixture (3). Here, the density function being approximated is assumed to be a Gaussian mixture given as follows

$$\widetilde{f}(\underline{x}_k^l, \underline{x}_k^n) = \sum_{j=1}^{N} w_k^j \mathcal{N}\left(\begin{bmatrix} \underline{x}_k^l \\ \underline{x}_k^n \end{bmatrix} - \begin{bmatrix} \underline{\mu}_k^{lj} \\ \underline{\mu}_k^{nj} \end{bmatrix}, \mathbf{C}_k^j \right) \quad , \qquad (8)$$

with the vectors $\underline{x}_k^l,\ \underline{\mu}_k^{lj} \in \mathbb{R}^r$ and $\underline{x}_k^n,\ \underline{\mu}_k^{nj} \in \mathbb{R}^s$. The weights w_k^j are all positive and add up to 1. Futhermore, the covariance matrices $\mathbf{C}_k^j \in \mathbb{R}^{(r+s)\times(r+s)}$ are given by

$$\mathbf{C}_k^j = \begin{bmatrix} \mathbf{C}_k^{lj} & \mathbf{C}_k^{lnj} \\ \mathbf{C}_k^{nlj} & \mathbf{C}_k^{nj} \end{bmatrix} \quad .$$

The density reapproximation step is a central part in the SGMF and essential for high quality estimation. Thus, a systematic and deterministic approximation procedure has to be chosen in order to reduce approximation errors.

The approximation is performed in two steps: First, the approximation of the marginal density in nonlinear subspace by a Dirac mixture density and then, the extension of the result to sliced Gaussian mixtures over the complete state space.

Approximation of nonlinear subspace For the approximation of the marginal density $\widetilde{f}(\underline{x}_k^n)$ by a Dirac mixture density (4), a systematic approximation approach is important. Using deterministic algorithms that minimize a certain distance measure, better approximation results can be achieved and fewer Dirac components are needed in comparison to random sampling. For the sliced Gaussian mixture representation, this results in fewer slices.

Different algorithms for approximation can be employed. A sequential algorithm is described in [10], which is based on a reduction of a cumulative distance measure over all one-dimensional marginals. Other approximation methods for one-dimensional densities yield optimal results at the cost of higher runtime [11] whereas general multidimensional problems are excessively computationally demanding. In [2] and [3], a Gaussian is approximated by samples along the principal axes of the covariance matrix. This can be done very efficiently, but only single Gaussian components can be approximated in contrast to the complete Gaussian mixture $\widetilde{f}(\underline{x}_k^n)$, and thus, more sample points are needed. For efficient approximation of a Gaussian density with several components, the method presented in [10] is used in this paper.

The approximation quality between the given Gaussian mixture density and the sliced Gaussian mixture approximation can be evaluated by certain distance measures, e.g., the Cramér-von Mises distance based on the localized cumulative distribution [12]. By defining a threshold, the number of slices can be increased, until the desired approximation quality is obtained. Thus, it is guaranteed that the approximation remains sufficient while always using the minimum number of slices needed.

Table 3: Parameters of the conditional Gaussian mixture density in linear subspace at slice position $\underline{\xi}_k^i$.

Conditionally linear subspace
$\beta_k^{ij} \leftarrow \frac{1}{b} w_k^j \mathcal{N}\left(\underline{\xi}_k^i - \underline{\mu}_k^{nj}, \mathbf{C}_k^{nj}\right)$
$\underline{\mu}_k^{lij} \leftarrow \underline{\mu}_k^{lj} + \mathbf{K}\left(\underline{\xi}_k^i - \underline{\mu}_k^{nj}\right)$
$\mathbf{C}_k^{lij} \leftarrow \mathbf{C}_k^{lj} - \mathbf{K}\mathbf{C}_k^{nj}\mathbf{K}^{\mathrm{T}}$
with $\quad b = \sum_{p=1}^{N} w_k^p \mathcal{N}\left(\underline{\xi}_k^i - \underline{\mu}_k^{np}, \mathbf{C}_k^{np}\right)$
$\mathbf{K} = \mathbf{C}_k^{lnj}\left(\mathbf{C}_k^{nj}\right)^{-1}$

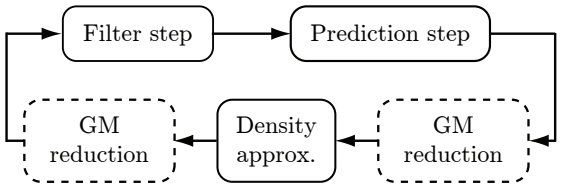

Figure 3: Processing steps of the SGMF.

Extension to complete state space $\widetilde{f}(\underline{x}_k^l | \underline{\xi}_k^i)$ denotes the resulting conditional Gaussian mixture density in linear subspace, determined by an evaluation of the true joint density $\widetilde{f}(\cdot)$ at the position $\underline{\xi}_k^i$ of the i-th Dirac impulse. So, this conditional density represents the i-th slice. The parameters of the conditional Gaussian mixture in linear subspace are calculated according to Table 3. By this means, the Gaussian mixture density $\widetilde{f}(\underline{x}_k^l, \underline{x}_k^n)$ can be efficiently and deterministically approximated by a sliced Gaussian mixture representation. The density reapproximation step is shown in Fig. 2.

3.4 Gaussian Mixture Reduction

For multiple processing steps in the Sliced Gaussian Mixture Filter, the number of overall Gaussian components increases with every density approximation. Let N_k be the number of Gaussian mixture components in the time step k and M the number of Dirac mixture components (slices). Then, $N_k = M \cdot N_{k-1} = M^{k-1} \cdot N_1$ since each slice consists of N_k Gaussian mixture components. In order to limit the exponentially increasing number of components, a component reduction on the individual slices is applied.

In general, the component reduction can take place before or after the density approximation. With a reduction before density approximation, a tradeoff between accuracy and execution time can be made. Component reduction after density approximation limits the maximum number of Gaussian components and thus, prevents exponential growth in computation time. The processing and possible component reduction steps are visualized in Fig. 3. Different approximation algorithms with a wide range of complexity and approximation quality exist, e.g., [13, 14, 15].

4 Cooperative Passive Tracking

A variety of passive sensors, e. g., infrared sensors, electro-optical sensors, ESM sensors, and jammed radar, delivers angular-only measurements. In such applications, estimation methods in general suffer from the fact that the range component of the state for a non-stationary target remains unobservable as long as the platform carrying the sensor is not maneuvering. One way to overcome this problem is a change of state space into non-Cartesian coordinates as, e. g., modified polar or log polar coordinates that effectively decouple the observable states from the non-observable ones, see [16] for a comparison.

Alternatively, observability can be achieved via so-called cooperative passive target tracking, i.e., by the use of several dislocated passive sensors. Then, one may apply, as a first possible approach, a Kalman filter based on pseudo-Cartesian measurements. These can be obtained from the angular measurements by triangulation, where various approaches to determine the corresponding covariance are known [17]. The resulting measurement model is a linear one. Such an approach is fairly simple, yet has to cope with possibly non-synchronous measurements from different sensors, missed detections, or problems arising if the target is close to the baseline formed by the sensors.

The problem of missed detections arises from the fact that the target detection probability of a real sensor is always $P_d < 1$. Thus, there may exist time steps, where at least one of the involved sensors cannot provide measurement data.

In contrast to the transformation of the angular measurements into Cartesian coordinates, one can, as a second approach, directly process the measured angles which leads to a nonlinear measurement model. However, this approach is more accurate and therefore chosen to be investigated in this paper.

As prerequisite for the measurement and system model discussed in the following subsections, the overall state vector is defined by $\underline{x}_k = [p_k, q_k, \dot{p}_k, \dot{q}_k, \omega_k]^{\mathrm{T}}$. It is decomposed into a linear substate $\underline{x}_k^l = [\dot{p}_k, \dot{q}_k]^{\mathrm{T}}$ representing the target's velocity and a nonlinear substate $\underline{x}_k^n = [p_k, q_k, \omega_k]^{\mathrm{T}}$ representing the target's position and turn rate. Note that we only consider the two-dimensional $[p, q]$ plane, i.e., the target's altitude is disregarded.

4.1 Measurement Model

For the measurement model, we assume that m sensors at positions

$$\underline{x}_S^{(i)} = \left[p_S^{(i)}, q_S^{(i)}\right]^{\mathrm{T}}, \quad i = 1, \ldots, m$$

take angular measurements originating from the target. Hence, at each time step k, a measurement $\hat{\underline{y}}_k$ consists of m angles

$$\hat{\underline{y}}_k = \left[\varphi_k^{(1)}, \ldots, \varphi_k^{(m)}\right]^{\mathrm{T}}$$

provided by the m sensors, respectively.

Referring to the measurement model given in (2), the measurement function $\underline{h}_k(\underline{\boldsymbol{x}}_k^n)$, which takes the nonlinear substate containing the target's position as input parameter, is given by

$$\underline{h}_k(\underline{\boldsymbol{x}}_k^n) = \left[h_k^{(1)}(\underline{\boldsymbol{x}}_k^n), \ldots, h_k^{(m)}(\underline{\boldsymbol{x}}_k^n)\right]^{\mathrm{T}}, \qquad (9)$$

where

$$h_k^{(i)}(\underline{\boldsymbol{x}}_k^n) = \operatorname{atan2}\left(\boldsymbol{q}_k - q_S^{(i)}, \boldsymbol{p}_k - p_S^{(i)}\right), \quad i = 1, \ldots, m \ .$$

$\operatorname{atan2}(y, x)$ is Matlab notation and defined as the angle between the positive x-axis and the point given by the coordinates $[x, y]^{\mathrm{T}}$. It can be recognized that there is no dependency on the linear substate $\underline{x}_k^l$ for angular measurements, so $\mathbf{H}_k(\underline{\boldsymbol{x}}_k^n) \equiv \mathbf{0}$.

Since the sensors act independently of each other, the measurement noise $\underline{\boldsymbol{v}}_k$ has a diagonal covariance matrix. If one or more sensors cannot deliver measurement data due to, e.g., missed detections, only the available data will be taken into account for the measurement function. Hence, the filter step operates with a reduced dimensionality of $\hat{\underline{y}}_k$ and $\underline{h}_k(\,\cdot\,)$.

4.2 System Model

As overall system model, we assume a *coordinated turn model*, which includes a *constant velocity model* with *white noise acceleration* for the straight motion [18]. Therefore, the state vector $\underline{x}_k$ contains an angular turn rate ω_k with $\omega_k > 0$ denoting a counterclockwise turn. Since it is part of the state vector, the turn rate is unknown and has to be estimated, which implies a nonlinear system model.

According to the investigated model, one has for the equations of motion in the $[p, q]$ plane $\ddot{p}_k = -\omega_k \dot{q}_k$ and $\ddot{q}_k = \omega_k \dot{p}_k$. We can now determine the system matrices for the linear and the nonlinear subspace by applying the coordinated turn model to the time-discrete system model (1) as follows:

$$\mathbf{A}_k^l(\underline{\boldsymbol{x}}_k^n) = \begin{bmatrix} \cos(\boldsymbol{\omega}_k T) & -\sin(\boldsymbol{\omega}_k T) \\ \sin(\boldsymbol{\omega}_k T) & \cos(\boldsymbol{\omega}_k T) \end{bmatrix}$$

and

$$\mathbf{A}_k^n(\underline{\boldsymbol{x}}_k^n) = \begin{bmatrix} T\,\mathrm{si}(\boldsymbol{\omega}_k T) & -T\,\mathrm{co}(\boldsymbol{\omega}_k T) \\ T\,\mathrm{co}(\boldsymbol{\omega}_k T) & T\,\mathrm{si}(\boldsymbol{\omega}_k T) \\ 0 & 0 \end{bmatrix},$$

where $T = t_{k+1} - t_k$ denotes the duration of a time step. The si and the co function are defined by

$$\mathrm{si}(x) = \begin{cases} \frac{\sin x}{x}, & x \neq 0 \\ 1, & x = 0 \end{cases}, \ \mathrm{co}(x) = \begin{cases} \frac{1-\cos x}{x}, & x \neq 0 \\ 0, & x = 0 \end{cases}.$$

Notably, the system matrices depend on the nonlinear substate vector, more precisely merely the turn rate ω_k. For the general system functions $\underline{a}_k^l(\,\cdot\,)$ in the linear subspace and $\underline{a}_k^n(\,\cdot\,)$ in the nonlinear subspace, we obtain $\underline{a}_k^l(\underline{\boldsymbol{x}}_k^n) = \underline{0}$ and $\underline{a}_k^n(\underline{\boldsymbol{x}}_k^n) = \underline{\boldsymbol{x}}_k^n$.

Because of the white noise acceleration assumption, the covariance of the system noise is given by

$$\mathbf{C}_k^w = \begin{bmatrix} \rho_k^2 \mathbf{Q}_0 & \mathbf{0}_{4\times 1} \\ \mathbf{0}_{1\times 4} & T^2 a_{\omega k}^2 \end{bmatrix},$$

where the factors ρ_k and $a_{\omega k}$ affect the acceleration of the translatory and the rotary motion, respectively. Furthermore,

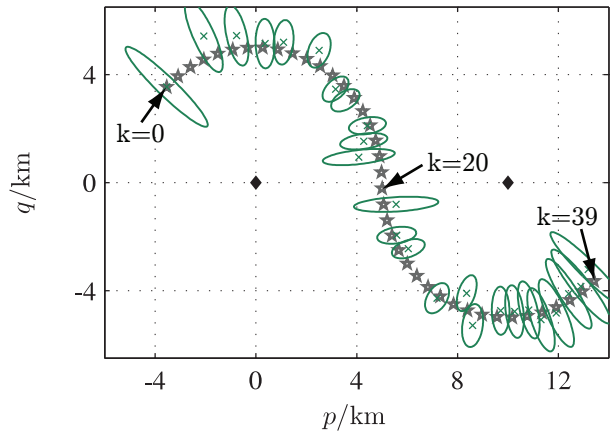

Figure 4: Illustration of cooperative passive target tracking with angular-only measurements: The target's true trajectory ($\star$) is tracked by two sensors at the displayed positions ($\blacklozenge$). Angular-only measurements are transformed to pseudo-Cartesian measurements with displayed means ($\times$) and covariances ($\circ$). Due to $P_d < 1$, triangulation is not possible in all time steps.

the matrix $\mathbf{Q}_0$ is given by

$$\mathbf{Q}_0 = \begin{bmatrix} T \cdot \mathbf{I}_2 & T^2/2 \cdot \mathbf{I}_2 \\ T^2/2 \cdot \mathbf{I}_2 & T^3/3 \cdot \mathbf{I}_2 \end{bmatrix} \ ,$$

where $\mathbf{I}_2$ denotes the 2×2 identity matrix. Note that the system noise includes correlation between the linear subspace and the nonlinear subspace, which is one of the main reasons for the extension of the Sliced Gaussian Mixture Filter.

5 Simulation Results

We consider a cooperative passive target tracking scenario as illustrated in Fig. 4: The target's true trajectory is an S-shaped curve shown as gray stars for time step $k = 0$ till time step $k = 39$. In order to initialize the simulation (see below) and to visualize the angular measurements along with their uncertainties, the measured angles and the measurement covariance are transformed to Cartesian coordinates by a triangulation-based method. These so-called *pseudo-Cartesian* measurements are displayed with green crosses and ellipses. Note that they are only used for visualization purposes as well as setup of the prior state and not during simulation runs. With a target detection probability of $P_d < 1$, there are cases where triangulation is not possible.

Example 1 (Simulation Setup)
In this first example, we consider two sensors, which take angular-only measurements, located at positions

$$\underline{x}_S^{(1)} = [0\ \text{km}, 0\ \text{km}]^{\mathrm{T}} \text{ and } \underline{x}_S^{(2)} = [10\ \text{km}, 0\ \text{km}]^{\mathrm{T}} \ .$$

Each sensor has a target detection probability of $P_d = 0.95$ and a measurement error with a standard deviation of $1.5°$. We choose the remaining parameters as follows: time step duration $T = 2$ s, initial target velocity $v_0 = 300$ m/s, $\rho_k^2 = 9.6236\ \text{m}^2\,\text{s}^{-3}$, and $a_{\omega k}^2 = 0.0144\ \text{s}^{-4}$.

The simulation is initialized in the following way: The position components of the prior density, which is Gaussian distributed, are equivalent to the pseudo-Cartesian measurement at time step $k = 0$. The velocity components are obtained by two-point differencing described in [18] and the turn rate is set to zero with a standard deviation of $45°/\text{s}$.

5.1 Marginal Density Representation

In Fig. 5, the estimation process with respect to Example 1 is illustrated. For the SGMF, we use 512 slices and for the MPF, we use 1024 and 2048 particles. Only the two-dimensional marginal density in the $[p, q]$ plane is depicted. The positions of the slices and particles before filtering are visualized as black dots. The re-weighted slices and particles after filtering are shown as orange dots; their size is determined according to the likelihood.

It can be seen from Fig. 5(a) that already a low number of slices is effectual to provide an accurate position estimate (shown as blue squares) with the SGMF. Although the number of particles is twice the number of slices, the distribution of the slices is more regular than the distribution of the particles shown in Fig. 5(b). For this example, at least 2048 particles are needed to provide a distribution which is similar to the distribution of the slices. This is illustrated in Fig. 5(c).

5.2 Estimation Performance

Two simulations for Example 1 have been carried out in order to present the estimation performance of the SGMF compared to the MPF illustrated in Fig. 6 and Fig. 7. The results for both simulations were obtained by 100 Monte Carlo runs, each one over 39 time steps. After density approximation, Gaussian mixture reduction has been applied using the algorithm described in [13].

First simulation In Fig. 6, the root mean square errors (RMSE) of the target's position, velocity and turn rate are shown for the SGMF using $M = 512$ slices (solid red lines) and the MPF using $2 \cdot M = 1024$ particles (dashed blue lines). Since a maximum of $N_k = 2$ Gaussian mixture components per slice has been chosen, the SGMF runs with up to $N_k \cdot M = 1024$ elementary components. Before density approximation, components with a small weight are discarded, so that 90% of the Gaussian mixture's probability mass is left. One can clearly see that the SGMF outperforms the MPF for position, velocity, and turn rate accuracy. The maximum near time step 20 in Fig. 6(a) is due to the fact that the target is close to the baseline formed by the two sensors.

Second simulation In Fig. 7, the RMSE of the target's position, velocity and turn rate are illustrated for the SGMF using $M = 256$ slices (solid red lines) with a maximum of $N_k = 5$ Gaussian mixture components per slice. Thus, up to $N_k \cdot M = 1280$ elementary components are used for the SGMF. As the MPF runs with $M = 2048$ particles (dashed blue lines) each one attached with a single Gaussian density in the linear subspace, less elementary components are employed for the SGMF. Nevertheless, the performance of the SGMF is superior compared to the performance of the MPF especially regarding the position error in Fig. 7(a).

The improved performance is due to the systematic and deterministic approach of the SGMF, which has advantages

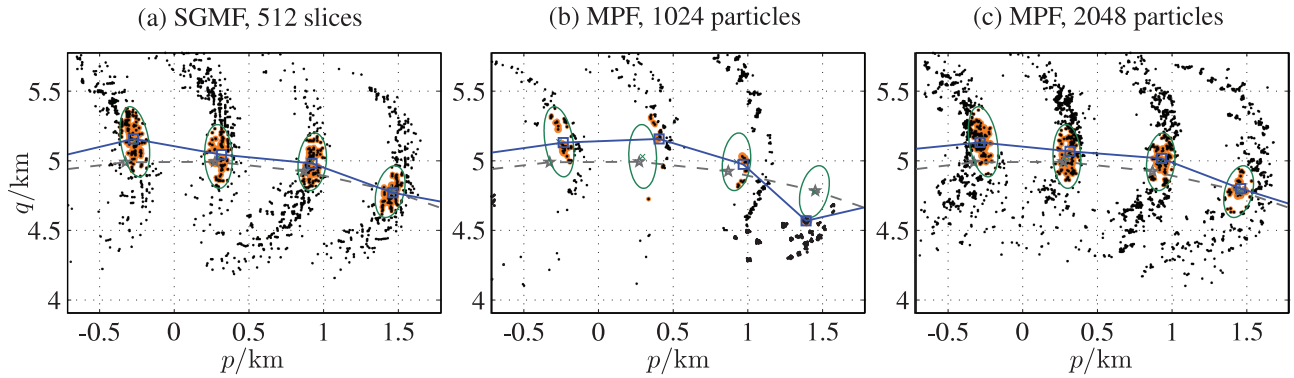

Figure 5: Visualization of density approximation and filtering: Measurement means (×) and covariances (○), Dirac mixture before filtering (●), re-weighted Dirac mixture after filtering (●), true positions (⋆, – –), and estimated trajectories (□, —) using (a) SGMF with 512 slices, (b) MPF with 1024 particles, and (c) MPF with 2048 particles.

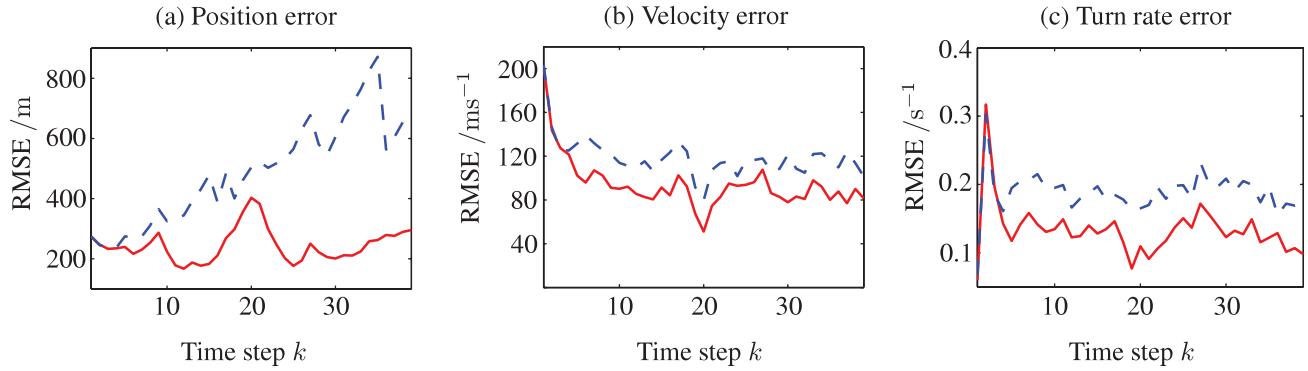

Figure 6: RMSE of (a) position, (b) velocity, and (c) turn rate based on 100 Monte Carlo simulations and a target detection probability of $P_d = 0.95$ for SGMF using 512 slices (—) and MPF using 1024 particles (– –).

compared to a randomized one, especially when using a similar number of samples.

6 Conclusion and Future Work

In this paper, the estimation of nonlinear systems with conditionally linear substructures by means of the Sliced Gaussian Mixture Filter was shown. A special density representation, the sliced Gaussian mixture density, allows the exact solution of the filter and prediction step. The deterministic and systematic approximation of arbitrary Gaussian mixture densities by sliced Gaussian mixture densities allows better approximations by using less components compared to random sampling.

The extensions of the proposed estimator in this paper include correlated system noise over the complete state space and an enhanced system model. Furthermore, the density approximation was applied to multi-dimensional nonlinear subspaces. All these extensions allow a much wider variety of applications of the filter.

In the application of cooperative passive target tracking, the SGMF is compared to the marginalized particle filter. Simulations show better estimation performance due to the systematic density re-approximation and the exact solution of the prediciton step.

Future work includes the combination of density approximation and the filter step. This allows approximation of the estimated density after the filter step, which can reduce the number of needed components for density approximation and can prevent degeneration. Such degeneration can occur, if the likelihood has only few or no mutual support with the prior density slices. Another extension is the application to completely nonlinear models by linearization of weakly nonlinear parts, which can be accomplished by the extended Kalman filter in a straightforward manner.

Acknowledgement

The authors thank Marco Huber for fruitful discussion and for providing the implementation of the Gaussian mixture reduction algorithm.
This work was partially supported by the German Research Foundation (DFG) within the Research Training Group GRK 1194 “Self-organizing Sensor-Actuator-Networks”.

References

[1] B. Ristic and M. S. Arulampalam, “Tracking a manoeuvring target using angle-only measurements: algorithms and performance,” *Signal Processing*, vol. 83, no. 6, pp. 1223–1238, Jan. 2003.

[2] S. J. Julier and J. K. Uhlmann, “Unscented Filtering and Nonlinear Estimation,” in *Proceedings of the IEEE*, vol. 92, no. 3, 2004, pp. 401–422.

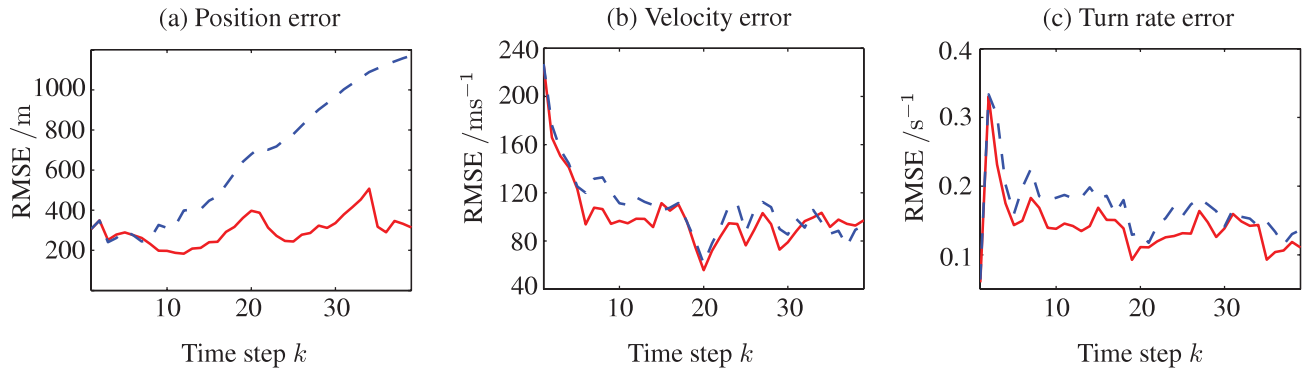

Figure 7: RMSE of (a) position, (b) velocity, and (c) turn rate based on 100 Monte Carlo simulations and a target detection probability of $P_d = 0.95$ for SGMF using 256 slices (—) and MPF using 2048 particles (– –).

[3] M. F. Huber and U. D. Hanebeck, "Gaussian Filter based on Deterministic Sampling for High Quality Nonlinear Estimation," in *Proceedings of the 17th IFAC World Congress (IFAC 2008)*, Seoul, Korea, Jul. 2008.

[4] M. S. Arulampalam, S. Maskell, N. Gordon, and T. Clapp, "A Tutorial on Particle Filters for Online Nonlinear/Non-Gaussian Bayesian Tracking," *IEEE Transactions on Signal Processing*, vol. 50, no. 2, pp. 174–188, Feb. 2002.

[5] V. Klumpp, F. Sawo, U. D. Hanebeck, and D. Fränken, "The Sliced Gaussian Mixture Filter for Efficient Nonlinear Estimation," in *Proceedings of the 11th International Conference on Information Fusion (Fusion 2008)*, Cologne, Germany, Jul. 2008.

[6] T. Schön, F. Gustafsson, and P.-J. Nordlund, "Marginalized Particle Filters for Mixed Linear/Nonlinear State-Space Models," *IEEE Transactions on Signal Processing*, vol. 53, no. 7, pp. 2279–2287, Jul. 2005.

[7] F. Sawo, V. Klumpp, and U. D. Hanebeck, "Simultaneous State and Parameter Estimation of Distributed-Parameter Physical Systems based on Sliced Gaussian Mixture Filter," in *Proceedings of the 11th International Conference on Information Fusion (Fusion 2008)*, Cologne, Germany, Jul. 2008.

[8] M. S. Arulampalam, B. Ristic, N. Gordon, and T. Mansell, "Bearings-Only Tracking of Manoeuvring Targets Using Particle Filters," *EURASIP Journal on Applied Signal Processing*, pp. 2351–2635, 2006.

[9] G. Casella and C. P. Robert, "Rao-Blackwellisation of Sampling Schemes," *Biometrika*, vol. 83, no. 1, pp. 81–94, 1996.

[10] V. Klumpp and U. D. Hanebeck, "Dirac Mixture Trees for Fast Suboptimal Multi-Dimensional Density Approximation," in *Proceedings of the 2008 IEEE International Conference on Multisensor Fusion and Integration for Intelligent Systems (MFI 2008)*, Seoul, Republic of Korea, Aug. 2008.

[11] O. C. Schrempf, D. Brunn, and U. D. Hanebeck, "Dirac Mixture Density Approximation Based on Minimization of the Weighted Cramér-von Mises Distance," in *Proceedings of the 2006 IEEE International Conference on Multisensor Fusion and Integration for Intelligent Systems (MFI 2006)*, Heidelberg, Germany, Sep. 2006, pp. 512–517.

[12] U. D. Hanebeck and V. Klumpp, "Localized Cumulative Distributions and a Multivariate Generalization of the Cramér-von Mises Distance," in *Proceedings of the 2008 IEEE International Conference on Multisensor Fusion and Integration for Intelligent Systems (MFI 2008)*, Seoul, Republic of Korea, Aug. 2008.

[13] M. West, "Approximating Posterior Distributions by Mixtures," *Journal of the Royal Statistical Society: Series B*, vol. 55, no. 2, pp. 409–422, 1993.

[14] A. R. Runnalls, "Kullback-Leibler Approach to Gaussian Mixture Reduction," *IEEE Transactions on Aerospace and Electronic Systems*, vol. 43, no. 3, pp. 989–999, Jul. 2007.

[15] M. F. Huber and U. D. Hanebeck, "Progressive Gaussian Mixture Reduction," in *Proceedings of the 11th International Conference on Information Fusion (Fusion 2008)*, Cologne, Germany, Jul. 2008.

[16] B. La Scala and M. Morelande, "An Analysis of the Single Sensor Bearings-Only Tracking Problem," in *Proceedings of the Eleventh International Conference of Information Fusion*, 2008, pp. 525–530.

[17] J. N. Sanders-Reed, "Error Propagation in Two-Sensor 3D Position Estimation," *Optical Engineering*, vol. 40, pp. 627–636, 2001.

[18] Y. Bar-Shalom and X. R. Li, *Estimation and Tracking: Principles, Techniques, and Software*. Artech House, Inc., Norwood, MA, USA, 1993.